NASA/TM—2006-214447

High Power High Efficiency Ka-Band Power Combiners for Solid-State Devices

Jon C. Freeman and Edwin G. Wintucky
Glenn Research Center, Cleveland, Ohio

Christine T. Chevalier
Analex Corporation, Brook Park, Ohio

November 2006

NASA STI Program . . . in Profile

Since its founding, NASA has been dedicated to the advancement of aeronautics and space science. The NASA Scientific and Technical Information (STI) program plays a key part in helping NASA maintain this important role.

The NASA STI Program operates under the auspices of the Agency Chief Information Officer. It collects, organizes, provides for archiving, and disseminates NASA's STI. The NASA STI program provides access to the NASA Aeronautics and Space Database and its public interface, the NASA Technical Reports Server, thus providing one of the largest collections of aeronautical and space science STI in the world. Results are published in both non-NASA channels and by NASA in the NASA STI Report Series, which includes the following report types:

- TECHNICAL PUBLICATION. Reports of completed research or a major significant phase of research that present the results of NASA programs and include extensive data or theoretical analysis. Includes compilations of significant scientific and technical data and information deemed to be of continuing reference value. NASA counterpart of peer-reviewed formal professional papers but has less stringent limitations on manuscript length and extent of graphic presentations.

- TECHNICAL MEMORANDUM. Scientific and technical findings that are preliminary or of specialized interest, e.g., quick release reports, working papers, and bibliographies that contain minimal annotation. Does not contain extensive analysis.

- CONTRACTOR REPORT. Scientific and technical findings by NASA-sponsored contractors and grantees.

- CONFERENCE PUBLICATION. Collected papers from scientific and technical conferences, symposia, seminars, or other meetings sponsored or cosponsored by NASA.

- SPECIAL PUBLICATION. Scientific, technical, or historical information from NASA programs, projects, and missions, often concerned with subjects having substantial public interest.

- TECHNICAL TRANSLATION. English-language translations of foreign scientific and technical material pertinent to NASA's mission.

Specialized services also include creating custom thesauri, building customized databases, organizing and publishing research results.

For more information about the NASA STI program, see the following:

- Access the NASA STI program home page at *http://www.sti.nasa.gov*

- E-mail your question via the Internet to *help@sti.nasa.gov*

- Fax your question to the NASA STI Help Desk at 301–621–0134

- Telephone the NASA STI Help Desk at 301–621–0390

- Write to:
  NASA STI Help Desk
  NASA Center for AeroSpace Information
  7121 Standard Drive
  Hanover, MD 21076–1320

NASA/TM—2006-214447

High Power High Efficiency Ka-Band Power Combiners for Solid-State Devices

Jon C. Freeman and Edwin G. Wintucky
Glenn Research Center, Cleveland, Ohio

Christine T. Chevalier
Analex Corporation, Brook Park, Ohio

National Aeronautics and
Space Administration

Glenn Research Center
Cleveland, Ohio 44135

November 2006

Acknowledgments

The authors would like to thank Dr. Rainee Simons for the support and encouragement for the work reported here.

Level of Review: This material has been technically reviewed by technical management.

Available from

NASA Center for Aerospace Information
7121 Standard Drive
Hanover, MD 21076–1320

National Technical Information Service
5285 Port Royal Road
Springfield, VA 22161

Available electronically at http://gltrs.grc.nasa.gov

High Power High Efficiency Ka-Band Power Combiners for Solid-State Devices

Jon C. Freeman and Edwin G. Wintucky
National Aeronautics and Space Administration
Glenn Research Center
Cleveland, Ohio 44135

Christine T. Chevalier
Analex Corporation
Brook Park, Ohio 44142

I. Introduction

Future manned and unmanned deep space exploration missions are envisioned that may require high efficiency, high power Ka-band space borne communication systems capable of data transmission rates of 1 Gbps and possibly more. Microwave transmitter powers in the range of 1 to 10 kW may be needed, depending on antenna size and configuration. High electrical efficiency is also desirable in order to maximize use of available electrical power and minimize heat dissipation requirements. The Ka-bands of interest are the current Deep Space Network (DSN) frequency band of 31.8 to 32.3 GHz and potentially the higher frequency band of 37 to 38 GHz. Vacuum electron devices such as traveling wave tubes (TWTs) are the only microwave amplifiers useful for space communications that are potentially capable of producing the required power and efficiency at these frequencies. However recently, solid-state power amplifiers (SSPAs) based on wide bandgap semiconductors (WBGS) such as, gallium nitride (GaN) have demonstrated high power capability and are therefore considered as replacements for vacuum electron devices. Hence, this report focuses on high power combiners for solid-state devices.

High Electron Mobility Transistors (HEMTs) fabricated from AlGaN/GaN heterojunctions are strong candidates for developing significant power (several watts) in the 20 to 40 GHz band. Table 1 summarizes the state-of-the-art (some of the recently published work 2001 to 2005) on these devices; the entries were developed from references 1 through 12. The values were obtained for on-wafer devices using load-pull measurements. Details on thermal and device reliability (slow drop in output power with time) are not available. One observes the saturated power is in the coarse range of 0.5 to 3.5 W per device. Figure 1 displays the power generation over the time interval, which shows the general trend of improved devices with time. The output power vs. frequency is shown in figure 2. The best entries at 30 and 35 GHz (ref. 10) are possible indicators of the drop-off of power with frequency. The power added efficiency (PAE) is depicted in figure 3; the highest value of 71 percent is indeed remarkable. One observes the trend of dropping PAE with frequency rather clearly. The variation of PAE with output power at 20, 30, and 40 GHz is given in figure 4; observe values between 20 and 35 percent are predominant. The gain at saturated output power is a key system parameter, and figure 5 elucidates the trends for HEMTs. In general one observes a gain between 5 and 10 dB. Figure 6 is illuminating, as it shows the improvement of developed power with total gate width (in mm). The devices from ref (ref. 10), which developed about 3.5 W, had 8 gates with a total gate width of 1.05 mm. More information on AlGaN/GaN HEMTs, is available in the special issue of IEEE Transactions on Microwave Theory and Techniques (ref. 13).

TABLE 1.—SUMMARY OF PERFORMANCE DATA FOR AlGaN/GaN HEMT POWER AMPLIFIERS OVER THE 20 TO 40 GHz FREQUENCY RANGE FROM THE INDICATED REFERENCES

Ref	f (GHz)	P(out) (W)	Gain (linear) (dB)	Gain (op) (dB)	PAE (%)	Year	Gate width (mm)
1	20	2	9.5	8	33	2002	0.5
2	20	1.6	12	10	27	2003	0.5
3	20	0.63	11	6	35	2001	0.1
4	20	0.44	9	5	71	2002	0.5
5	20	1.6	12	9	27	2002	0.5
6	30	1.6	5	5	17	2003	0.4
7	30	1.1	7	5	9	2002	0.72
7	35	0.91	6	4	9	2002	0.72
7	35	0.63	6	4	8	2002	0.48
7	35	0.48	5	3	6	2002	0.48
8	30	1.09	9	6.7	33	2003	0.2
8	35	0.826	7.5	5.5	23	2003	0.2
7	40	0.62	-	-	4	2002	0.72
9	30	1	8	7.5	45	2005	0.15
10	30	3.64	8	6	26	2003	1.05
10	35	3.45	7.5	4.9	22	2003	1.05
11	30	2.3	---	-	--	2002	0.36
12	40	1.58	6	4	33	2005	0.15

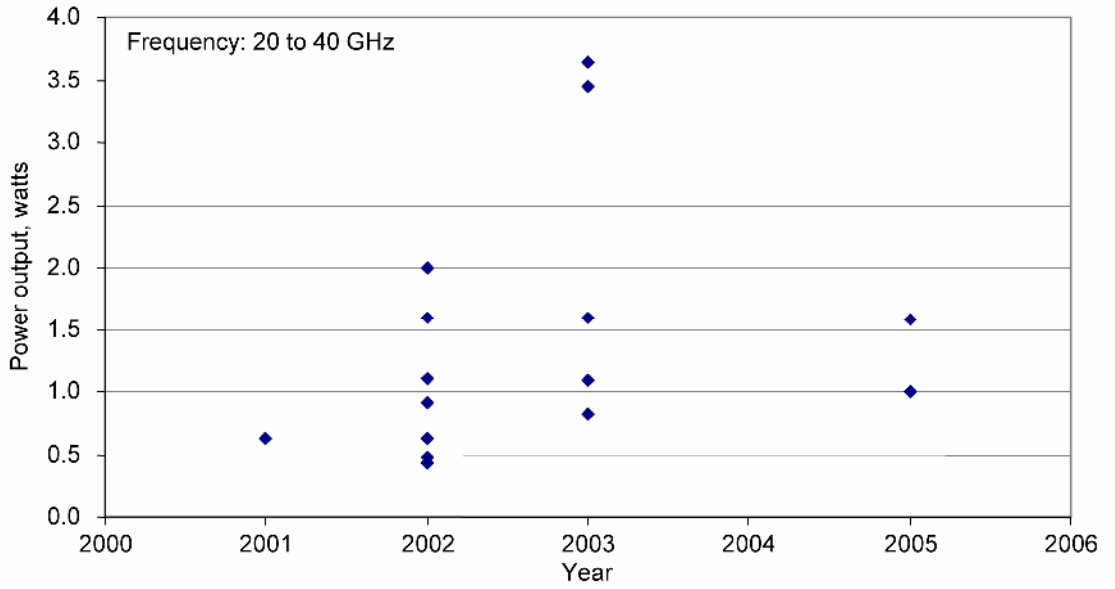

Figure 1.—Evolution of generated power from AlGaN/GaN amplifiers during the period from 2001 to 2005.

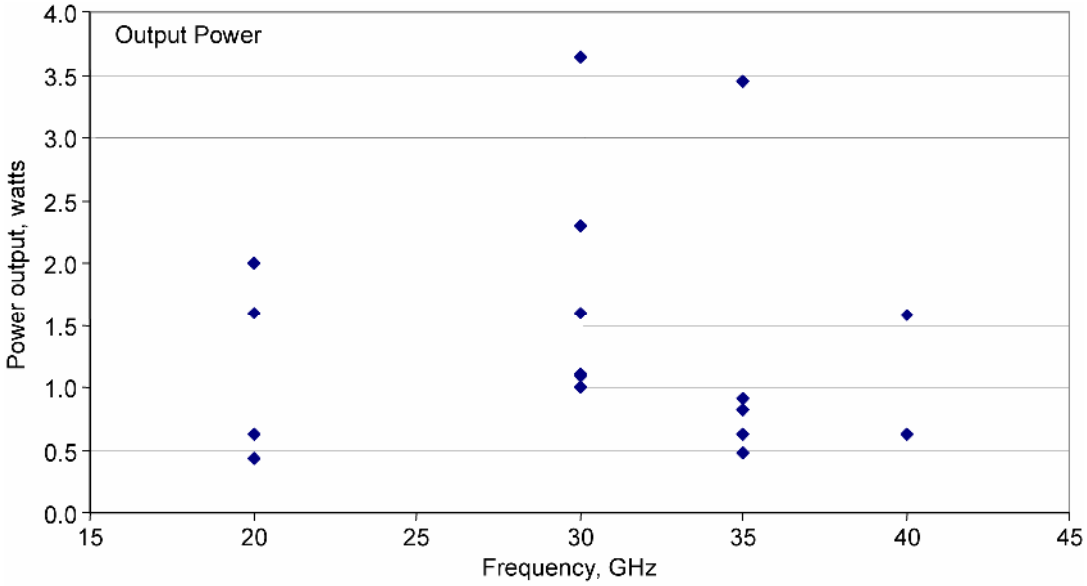

Figure 2.—Output power vs frequency across the 20 to 40 GHz band.

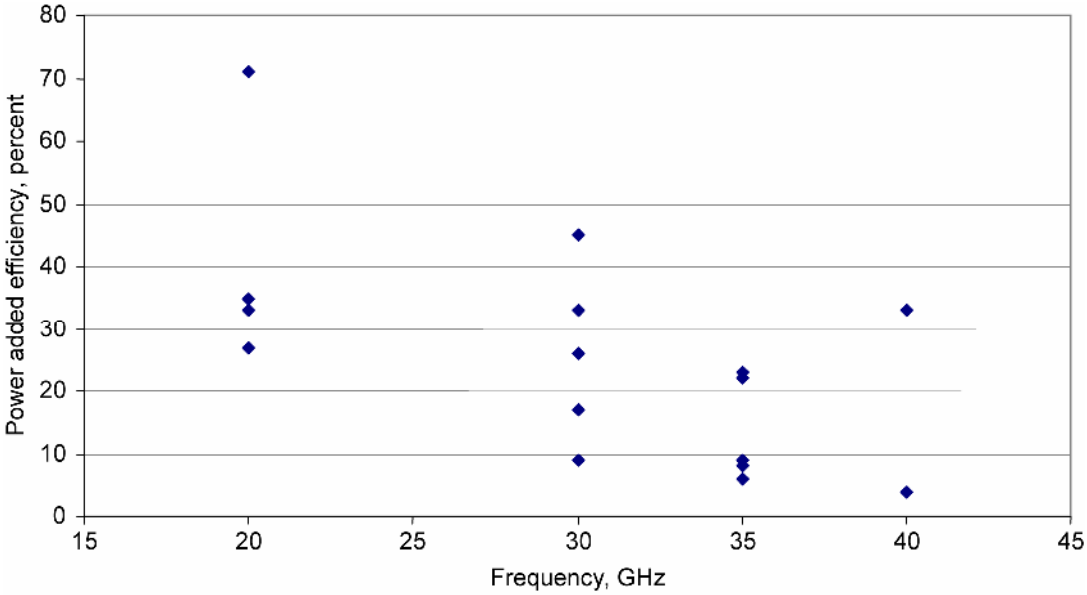

Figure 3.—Power added efficiency of AlGaN/GaN HEMT amplifiers from 20 to 40 GHz.

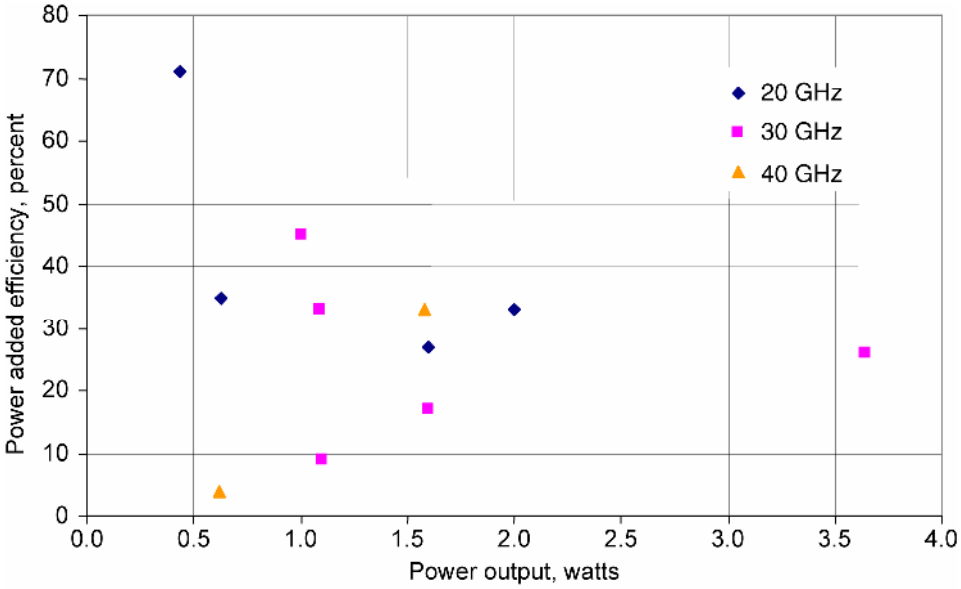

Figure 4.—Power Added Efficiency (PAE) versus output power at 20, 30, and 40 GHz.

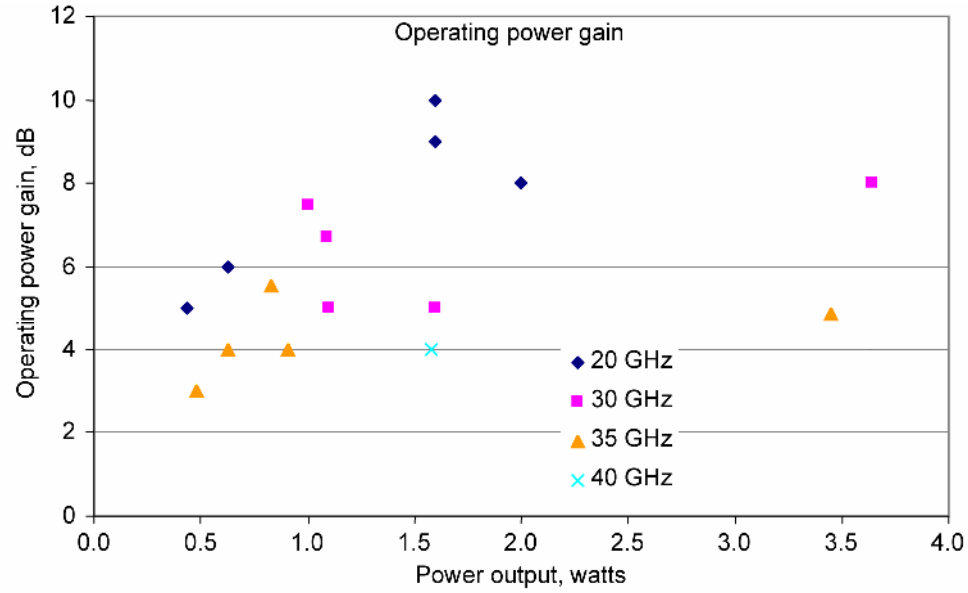

Figure 5.—Operating power gain G(oper.) as a function of output power from 20 to 40 GHz.

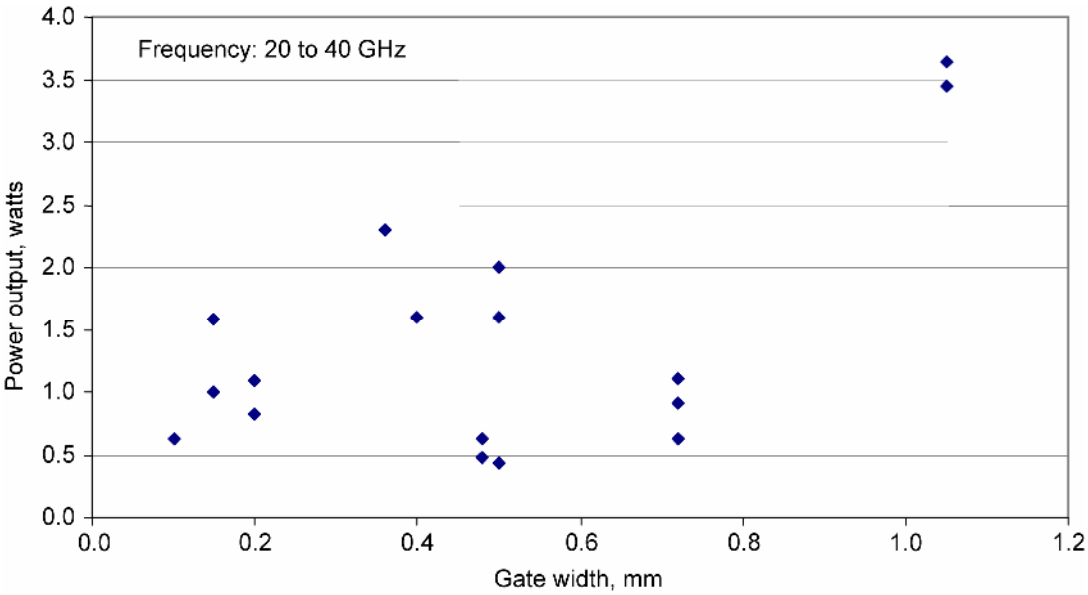

Figure 6.—Output power versus total gate width in mm.

II. Combiner Schemes

This report summarizes the results of a study conducted on high power high efficiency Ka-Band combiners for solid-state devices. Basically two types of combiners were investigated. The first combiner is based on short-slot couplers. The second combiner is based on magic-tees. The construction of the two combiners is described in the following sections and the computer modeled/simulated or experimental results are presented. The specifications for the SSPA are given in table 2.

TABLE 2.—SPECIFICATION FOR A Ka-BAND HIGH POWER HIGH EFFICIENCY SSPA

Center Frequency	32 GHz
Output Power	120 W CW
Power Added Efficiency	30% Minimum
Bandwidth	10%
AM/PM Conversion	2°/dB Max
Gain Compression	6dB Max
Css/No	122 dB-Hz
Noise Figure	20 dB Max
Phase Ripple	3° Max
Gain	50 dB Min
Gain Tilt	2 to 0 dB
Environment	Geosynchronous Orbit

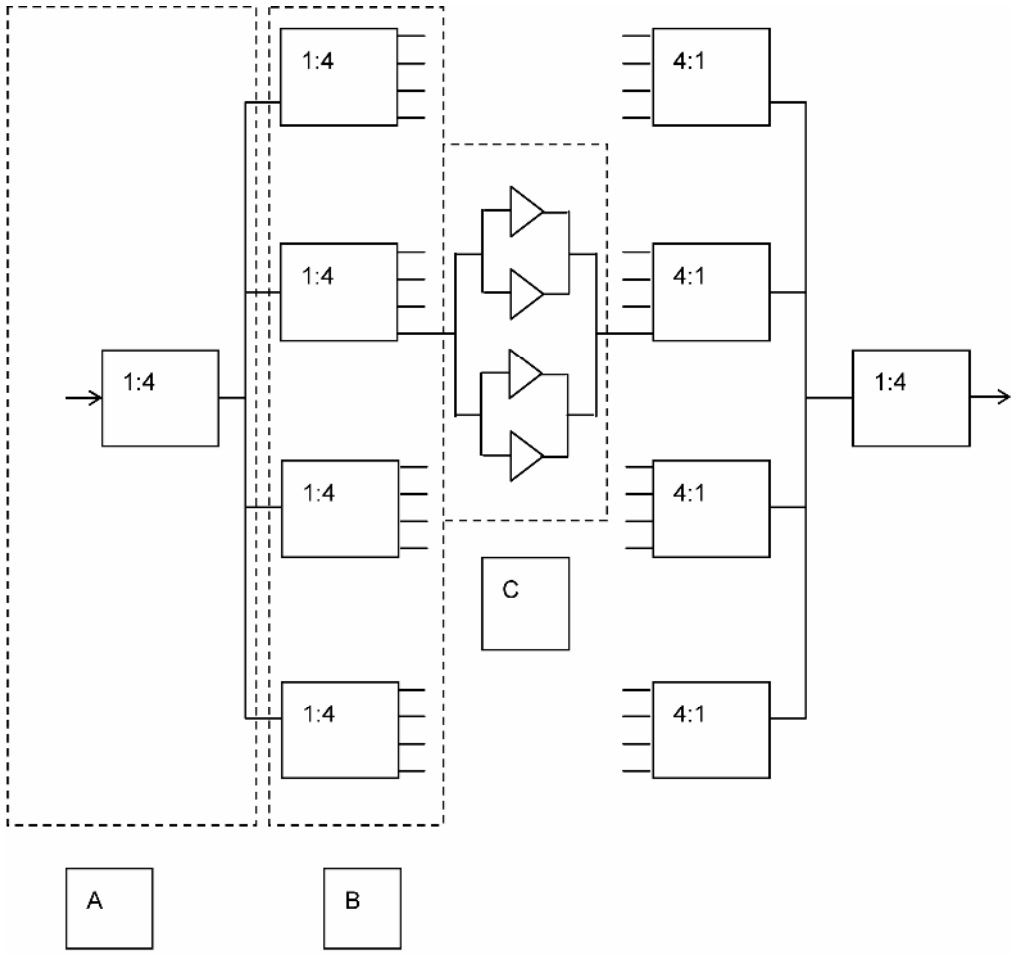

Figure 7.—Schematic of the 1:4 repeated scheme for power combining. The 1:4 unit in section A is comprised of three standard magic-Ts. The units in section B are comprised of short-slot couplers. Section C is reconfigurable; holding 4(as shown), 2, or 1 MMIC amplifiers.

III. Short-Slot Coupler Based Combiner

This combiner is based on short-slot couplers due to the inherent wideband nature of this form of coupler. The design goals are to develop a low-loss, modular, and low cost unit. The unit is centered at 28 GHz with a 6 GHz bandwidth, and is designed using the software package Microwave Studio. In contrast, commercially available short-slot and hybrid ring couplers have a bandwidth and insertion loss of about 3 GHz and 0.5 dB respectively at Ka-Band frequencies (ref. 14). The center frequency of 28 GHz was chosen to accommodate the commercially available TriQuint PHEMT packaged MMIC amplifier. However, this design can be extended to 32 GHz to meet the specifications listed in table 2. The combining of MMIC amplifiers for high power applications has received much attention in recent years (refs. 15, 16, and 17).

Figure 7 displays the basic 1:4 splitter/combiner concept based on short-slot couplers (ref. 18). The input 1:4 splitter in section A is formed with 3 waveguide magic-Tees. One such splitter will be discussed later in section VIII (b). Section B shows the four short-slot coupled assemblies. Each has four output ports. Section C denotes the GaN MMIC amplifier chip carrier section. Shown in section C are four MMIC amplifier units connected with Wilkinson combiners. By inspection, one sees that it is possible to combine up to 64 discrete MMIC amplifiers. By altering section C one may combine 32 or 16 discrete MMIC amplifiers. The output combining section is essentially the inverse of the input.

IV. Short-Slot Coupler Simulated Performance

Figure 8 shows the cascade of three short-slot couplers that constitute one of the four boxes in section B of figure 7. The three couplers are combined in non-standard oversized waveguide to obtain both wide bandwidth and low loss and is the main innovation in this effort. The inside dimensions of the oversized waveguide are 0.6589 by 0.4420 cm. A transformer to WR-28 is included on the input port. Figure 9 depicts the short-slot coupler. Labeling the ports as: port 1: input, port 2: isolated, ports 3 and 4, the coupled ones; the simulated S-parameters at the center frequency of 28 GHz for the loss free case are: S_{11} = –26.7 dB, S_{21} = –23.2 dB, S_{31} = –2.9 dB, and S_{41} = –3.2 dB. Figure 10 is similar to figure 8 with the top metal wall removed, while showing both upper and lower capacitive posts; which are collinear. The plot in figure 10 shows the simulated return loss (RL), which is better than 25 dB across the band. In addition, the ripple in the coupling levels at the four output ports is very small.

V. Combiner Fabrication and Layout

In figure 11 we display the manufacturer's drawing of the complete 1:4 splitter/combiner. Due to phasing and manufacturing constraints, the two units are not identical; for one thing, the terminations (shown in green) on the isolated ports are at different locations, and the capacitive coupling posts are on different sides of the centerline. The transformer sections facilitate the use of standard WR-28 waveguide-to-coax transitions. The coax ports attach to standard coax-to-microstrip transitions (not shown) located on the chip carrier unit. The chip carrier unit is inserted between the coax ports shown at the bottom of the drawing. Figure 12 displays the microstrip/chip carrier unit. For this effort, a single packaged MMIC amplifier from TriQuint (Model TGA 4905) is used. The four discrete amplifiers are isolated with the top cover.

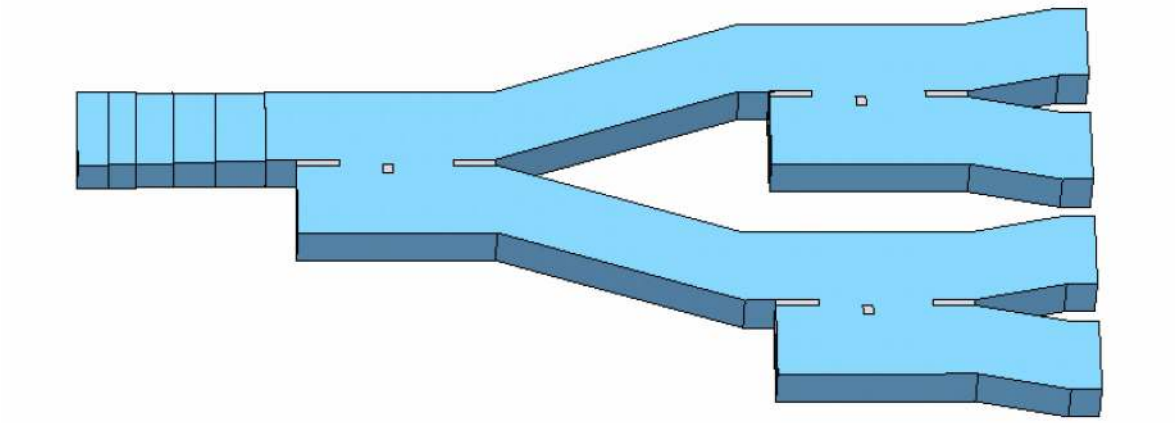

Figure 8.—The 1:4 configuration using a cascade of three short-slot couplers. The couplers and connecting waveguide are non-standard so a transformer to WR-28 waveguide is provided at the input. Transformers at the output ports are not shown.

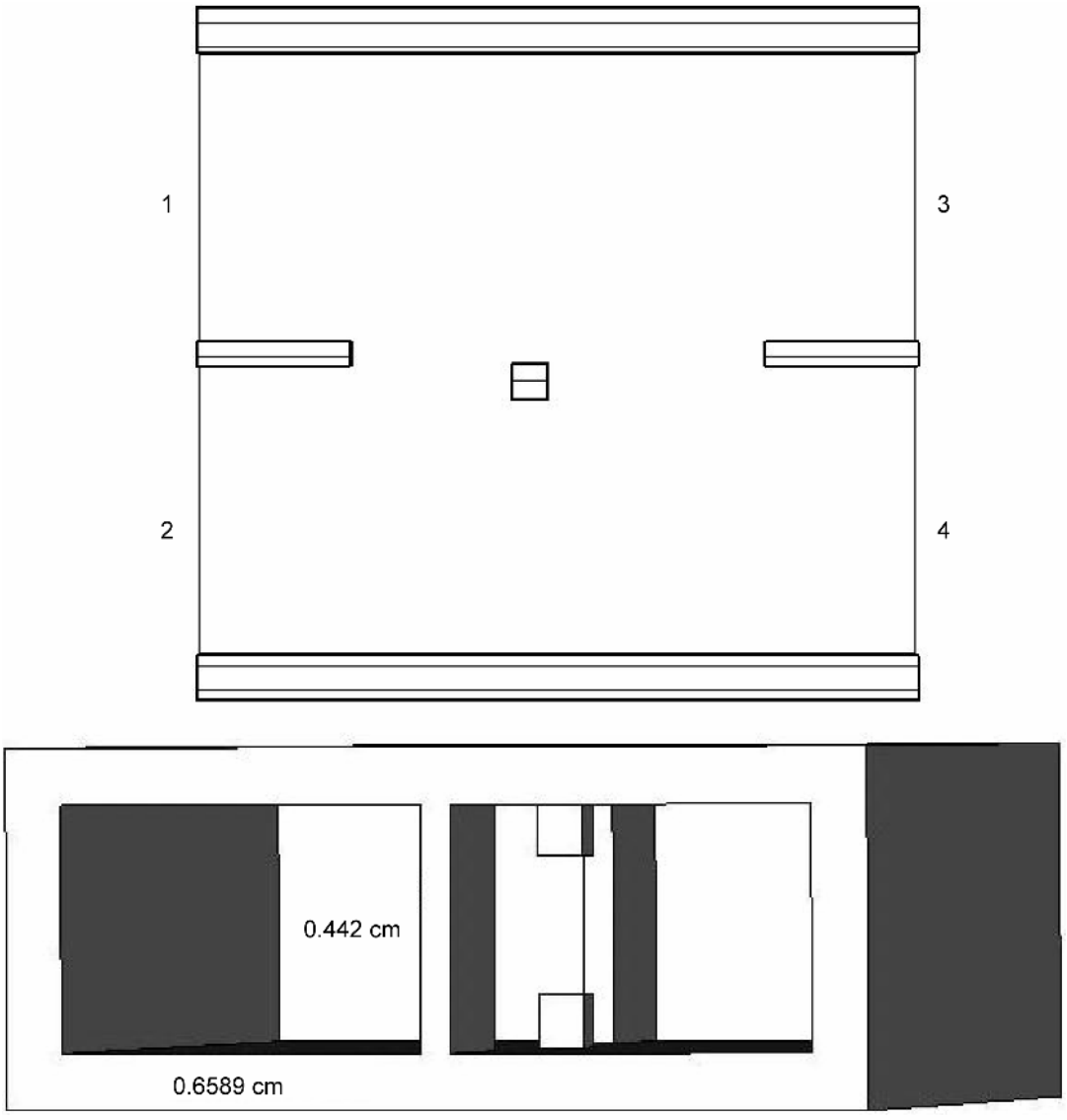

Figure 9.—Top and perspective view of the short-slot coupler. The capacitive coupling posts on the top and bottom walls of the waveguide are offset from the center line. In the perspective view ports 1 and 2 are to the left and right respectively. Ports 3 and 4 are partially obstructed.

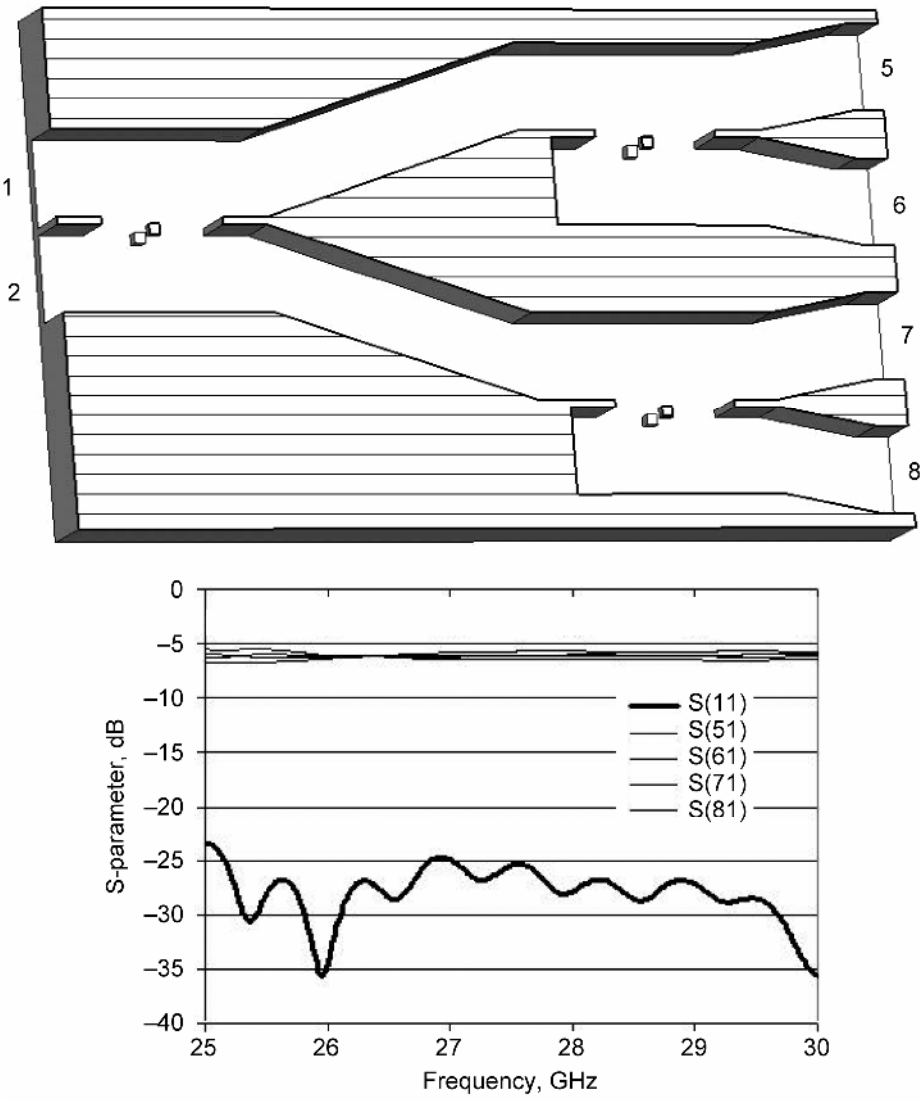

Figure 10.—1:4 splitter section with the top wall removed. Both capacitive posts are shown (those slightly to the right are on the top wall). The lower plot gives the return loss, (RL), S_{11} (heavy) and the transmissions to the output ports 5,6,7, and 8. From 25.5 to 30 GHz the RL is equal or better than 25 dB.

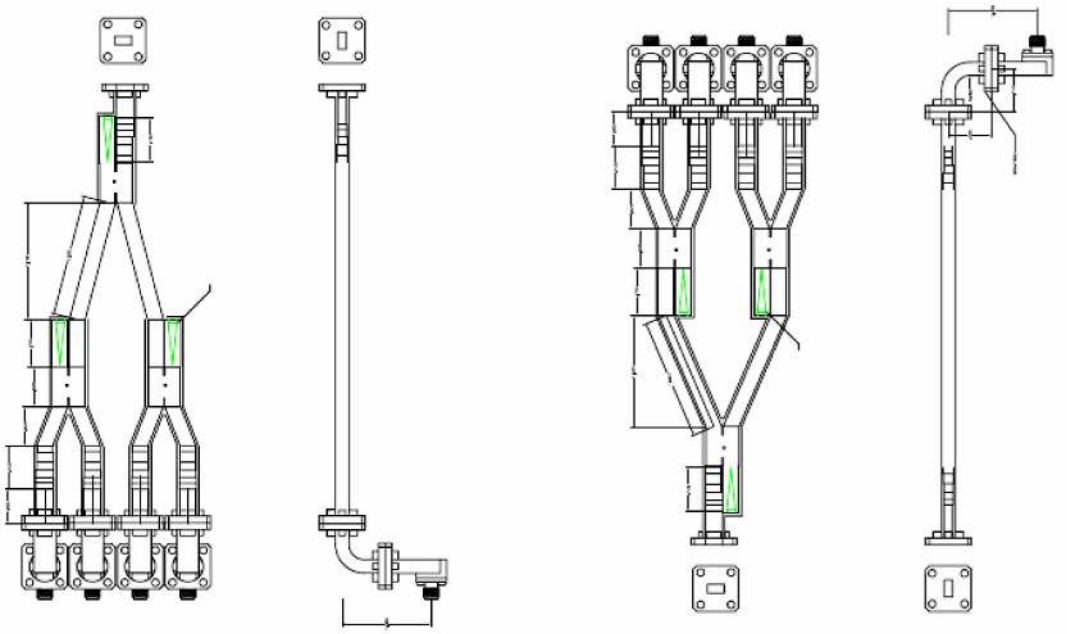

Figure 11.—Top and side views of the splitter/combiner sections. The distance between input and output flanges is about 12 inches. The microstrip/amplifier carrier unit goes between the sections.

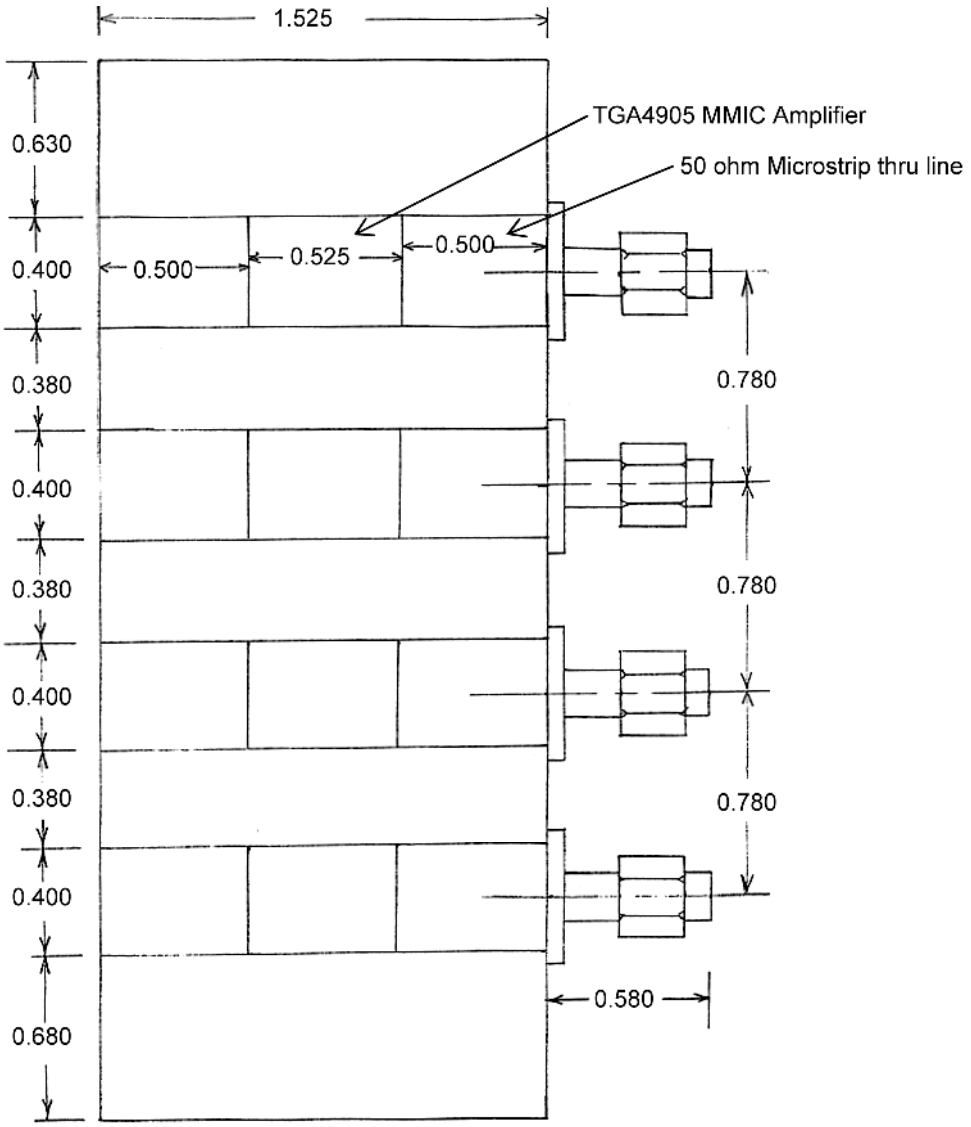

Figure 12.—The microstrip/chip carrier unit. Variable length input/output tiles are used to accommodate slightly different package dimensions of various amplifier modules. The unit also provides heat sinking and houses the power supply (not shown). Transitions on the left side are not shown.

VI. MMIC Amplifier Test Data

Figure 13 gives the input/output return losses and the output power of the TriQuint MMIC amplifier (Model TGA 4905) over the frequency band of interest. These results were obtained with the configuration shown in the lower part of figure 13. The amplifier package is coupled to input and output 50-Ω microstrip lines with 3 jumpers or bond wires. The measured return loss (RL) is in the –6 dB range; one observes that the amplifier is not well matched to 50 Ω. The terminations in the splitter side will absorb the reflected signal over the entire band (verified from simulation.)

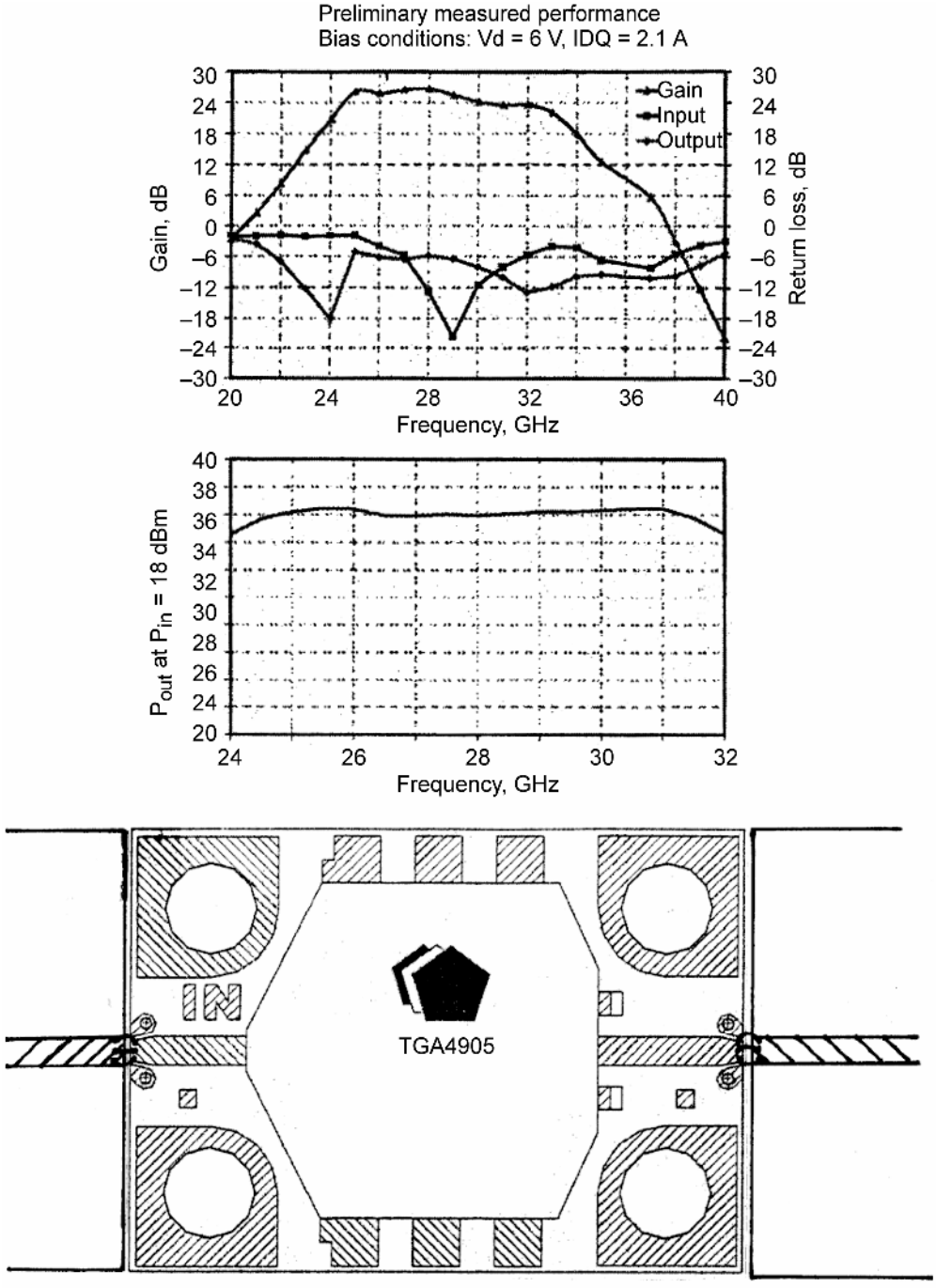

Figure 13.—Upper plots are TriQuint's representative gain, return loss, and output power over the 24 to 32 GHz band. Upwards of 3W are available over most of the band. The lower sketch shows the connection of the amplifier module to microstrip lines with 3 jumpers.

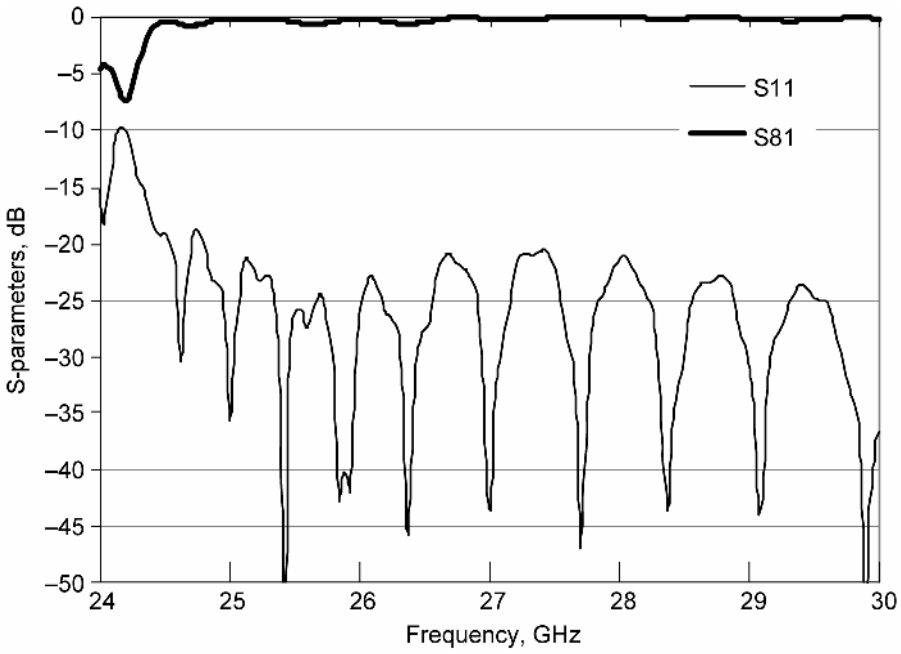

Figure 14.—The simulated transmission and RL of a splitter and combiner connected back-to-back. Waveguide loss corresponding to measured data was used in the calculation.

VII. Short-Slot Combiner Simulation Results

The simulated S-parameters at 28 GHz for the loss free case for the overall 1:4 splitter are S_{11} = –27.9 dB, S_{51} = –5.7 dB, S_{61} = –6.1 dB, S_{71} = –6.1 dB, and S_{81} = –6.4 dB. When the input and output sections were connected back-to-back with metal conductivity equaling 3.816 E+7 S/m (to correspond to measured loss in WR-28), we obtained return loss S_{11} = –21.9 dB and transmission loss S_{81} = –0.2 dB at the center frequency. The overall transmission and return loss are shown in figure 14.

The overall splitter/combiner was designed for low cost and maximum flexibility. It permits the combining of 16, 32, or 64 MMIC amplifiers over a broad band. It can accommodate packaged or unpackaged amplifying units of various dimensions with arbitrary input/output matching requirements. The overall length of the unit between input/output WR-28 waveguide flanges is approximately 12 in.. The estimated cost to manufacture four input/output units with the four MMIC amplifiers mounting structures is $65,736.00. Additional costs to form a complete power amplifier include the 32 WR-28 waveguide-to-coax-to-microstrip transitions, the microstrip tiles, power supply, and amplifier modules.

VIII. Magic-Tee Based Combiner

Two types of magic-tee based power combiners were investigated and figure 15(a) and (b) illustrate the configurations, respectively. In the configuration shown in figure 15(a), the two amplifiers whose output are to be combined are coupled to the E-plane and H-Plane ports which are orthogonal and along the plane of symmetry of the magic-tee. The advantage of this approach is the high isolation (>30 dB) that exists been these ports which de-couple the two amplifiers. Alternatively, the amplifiers can be coupled to the two co-linear H-plane ports as shown in figure 15(b). The advantage of this approach is lower profile and compactness, however the isolation between the input ports is low (~ 20 dB). The experimentally obtained results of both of these approaches are presented in the following sections.

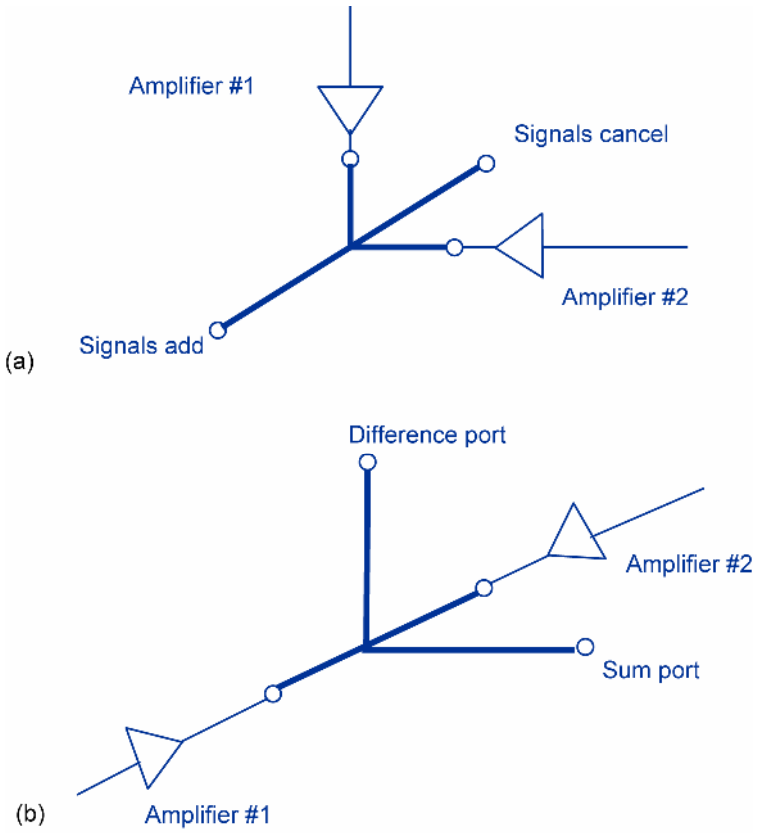

Figure 15.—Schematic of a Magic-Tee Based Two-Way Combiner. (a) Input ports are orthogonal. (b) Input ports are co-linear.

(a) Two-Way Combiner With Orthogonal Input Ports

The configuration for a two-way combiner (refs. 19 and 20) is shown in figure 16. The magic-tee is designed such that the input signals add in phase at one output (port no.2 in fig. 16) and cancel in phase at the other output (port no. 3 in fig. 16). Optimum performance as a power combiner therefore requires a balance of power and phase at the two input ports. The magic-tee allows efficient combining of the MMIC amplifiers in pairs as shown in figure 17. The electrical specifications of the magic-tee used in our experiments are presented in table 3. The actual magic-tee is presented in figure 18.

For the purpose of demonstrating the low loss high power handling capability of the magic-tee, two 100 W traveling wave tube amplifiers (TWTAs) operating over the frequency range of 31.8 to 32.3 GHz were used in place of the MMIC amplifiers. The power at the output port was about 180 W. The combining efficiency over 1 GHz band centered at 32.05 GHz is shown in figure 19. It is observed that the combining efficiency is as high as 90 percent, which translates to an insertion loss of about 0.5 dB for a two-way combiner. From these results it is evident that the magic-tee based combiner meets the high efficiency and high power requirements outlined in table 2. In addition, error-free data transmission at 8 Mbps (BPSK and QPSK) was also successfully demonstrated through the combiner.

(b) Four-Way Combiner With Co-linear Input Ports

The configuration for a four-way combiner is shown in figure 20. The four-way combiner is built using three magic-tees and makes use of split block construction for compactness as illustrated in figure 21. The measured input return loss S_{11} is presented in figure 22. The S_{11} is better than –12 dB across the 31.0 to 40.0 GHz band. The measured return loss at each of the output ports nos. 2 through 5 is

better than –23.0 dB across the 26.5 to 31.0 GHz frequency band. The measured transmission or insertion loss between port no. 1 and ports no. 2 through no. 5 (S_{21}, S_{31}, S_{41}, S_{51}) are presented in figures 23 through 26, respectively. The maximum insertion loss is about 0.63 dB across the 26.5 to 32.0 GHz band, which translates into a minimum combining efficiency of about 86.5 percent for a four-way combiner.

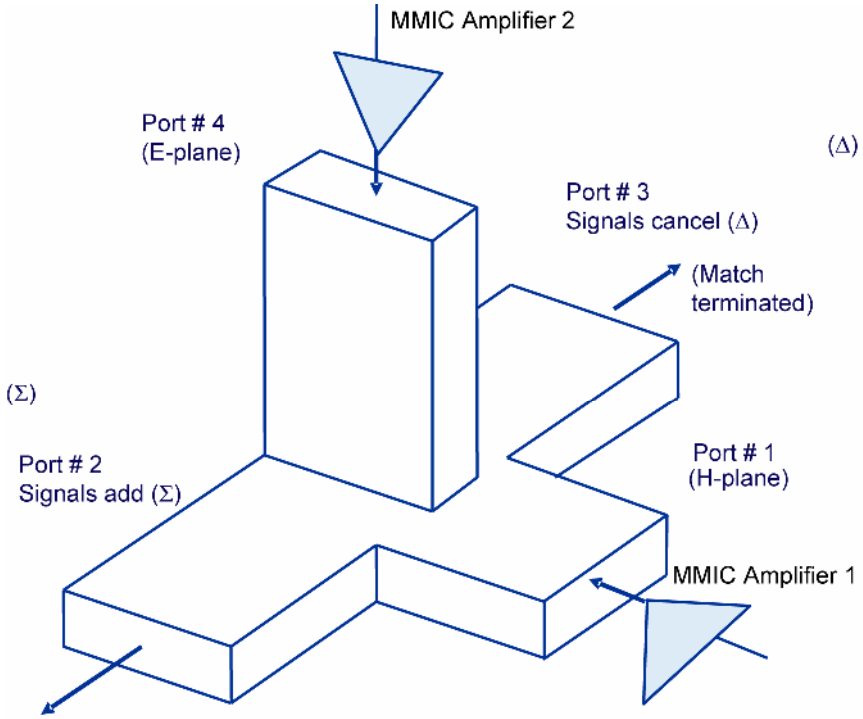

Figure 16.—Basic configuration of waveguide magic-T as a combiner for two microwave amplifiers

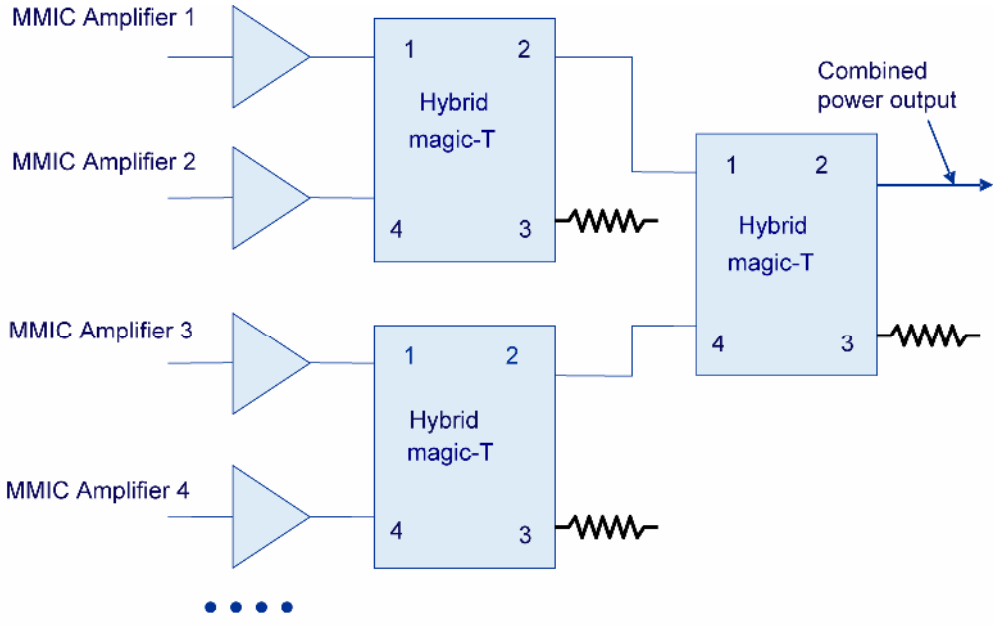

Figure 17.—Binary circuit architecture for combining 2^n amplifiers where n is an integer.

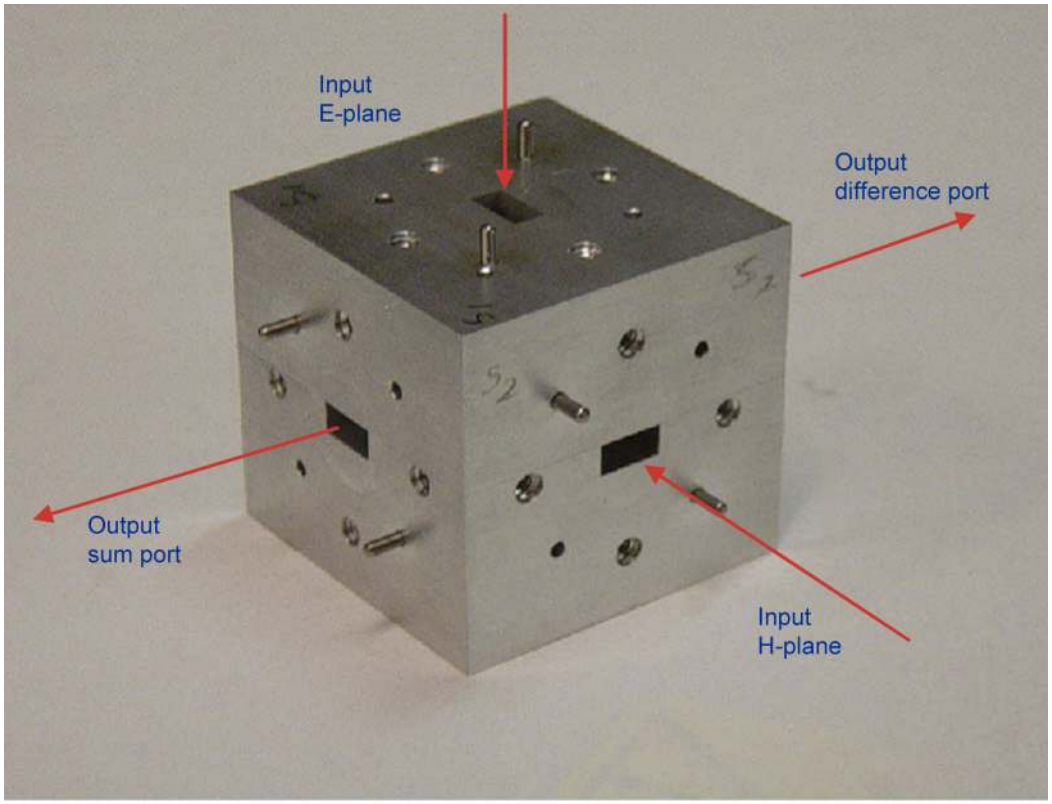

Figure 18.—4-port magic-T junction showing sum (inputs add in phase) and difference (inputs cancel in phase) output ports.

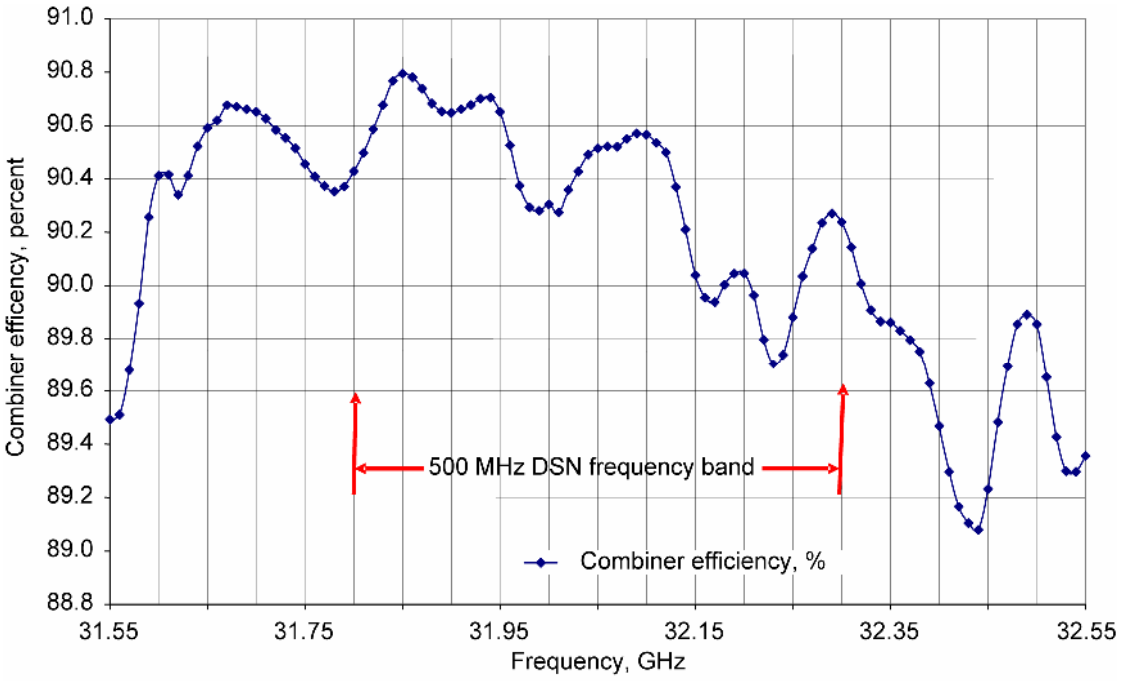

Figure 19.—Combiner efficiency over 1 GHz frequency band.

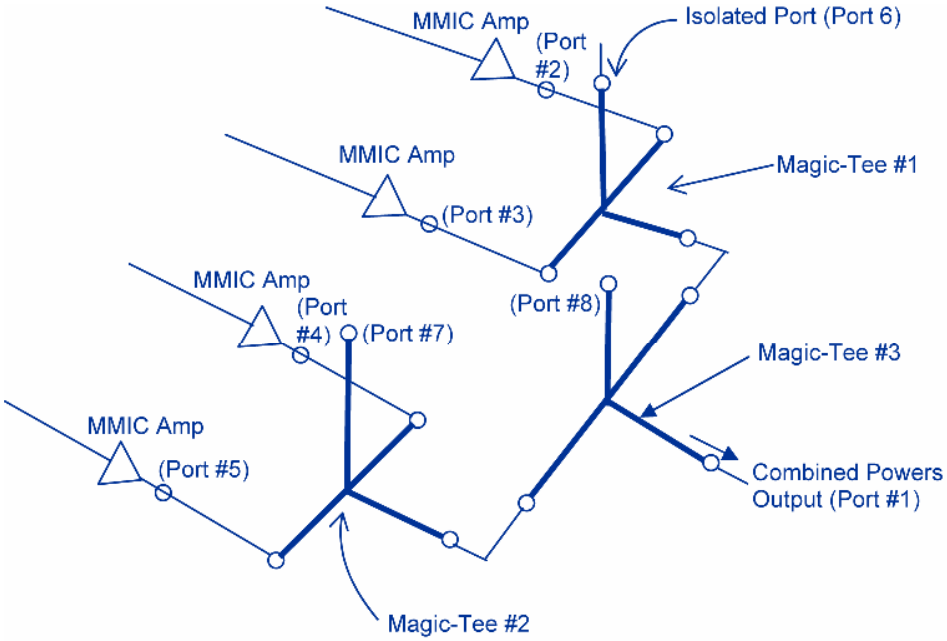

Figure 20.—Schematic of a Magic-Tee Based Four-Way Power Combiner.

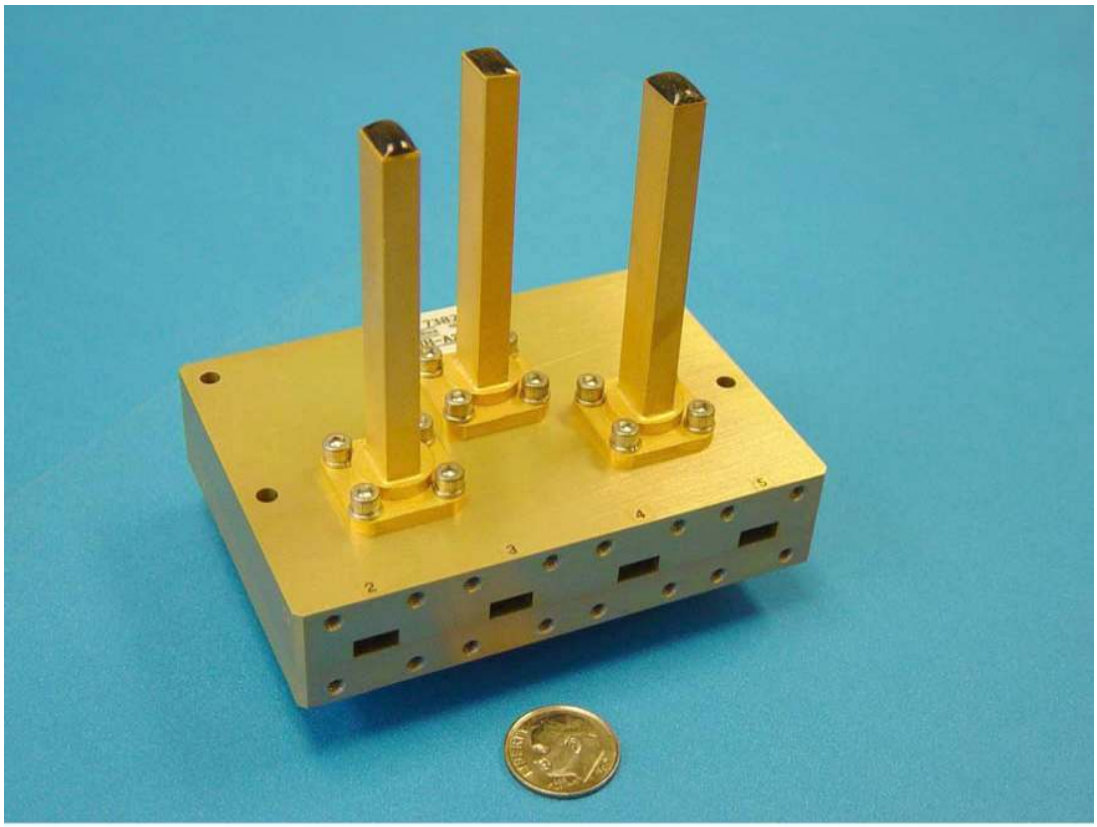

Figure 21.—Photograph of the 1 to 4 power splitter/combiner. It is configured with magic-Ts as shown in Figure 20. It consists of a cascade of 3 individual magic-T's. The ports visible are ports #2 to #5 of Figure 20. The terminated ports are #6 to #8 (three shown on the top). The combined port on the back (not shown) corresponds to port #1 in Figure 20.

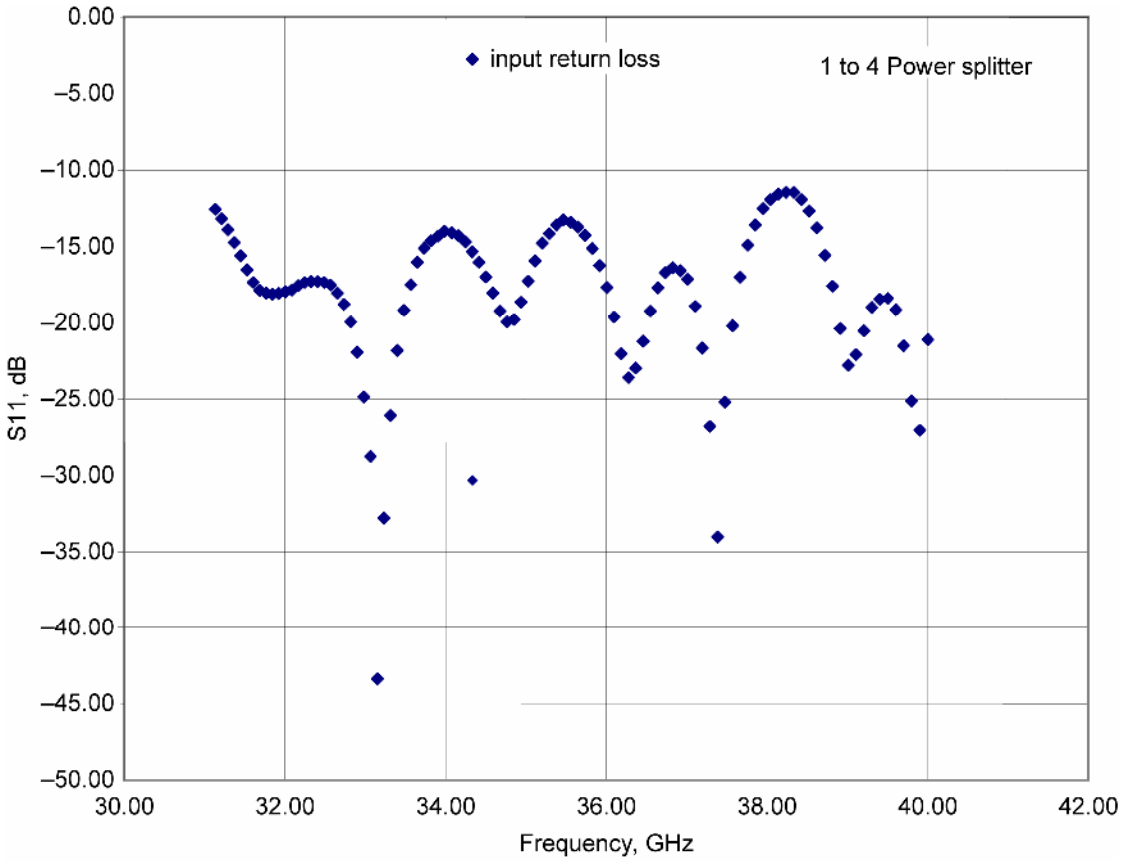

Figure 22.—The measured input return loss (S11) (RL) of the power splitter. The RL of each of the output ports (S22, S33, S44, S55) was better than 23 dB.

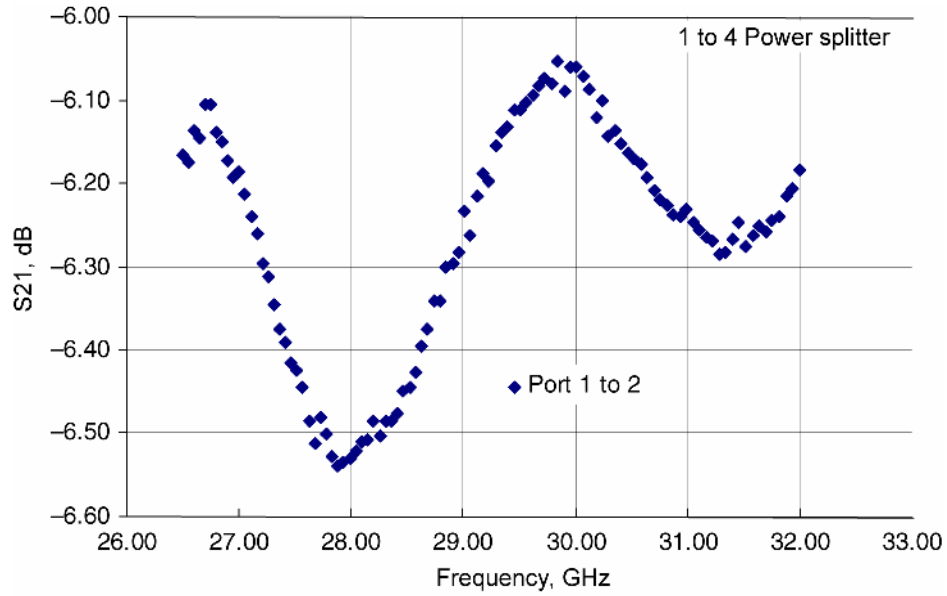

Figure 23.—The measured transmission to port #2. Narrow band sweep.

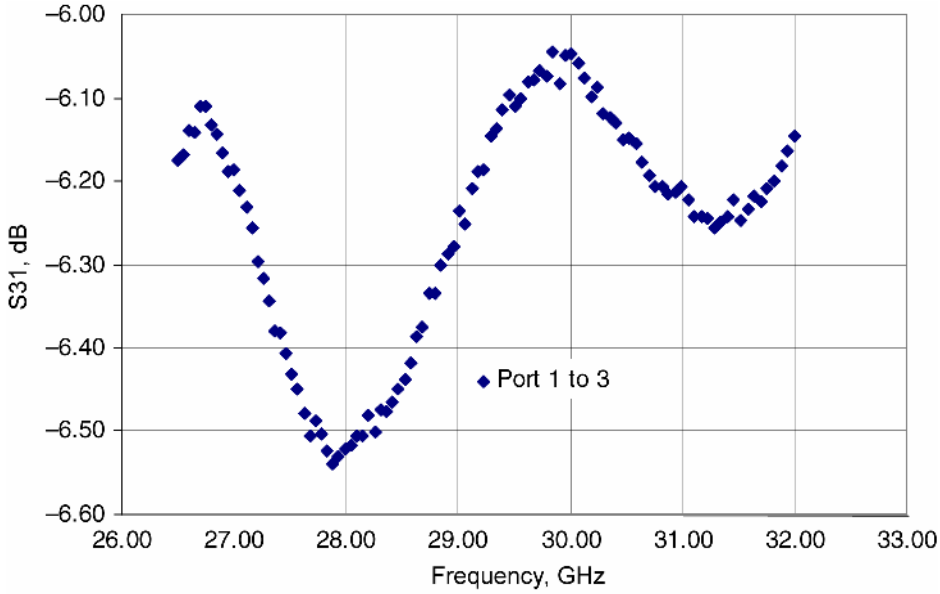

Figure 24.—The measured transmission to port #3. Narrow band sweep.

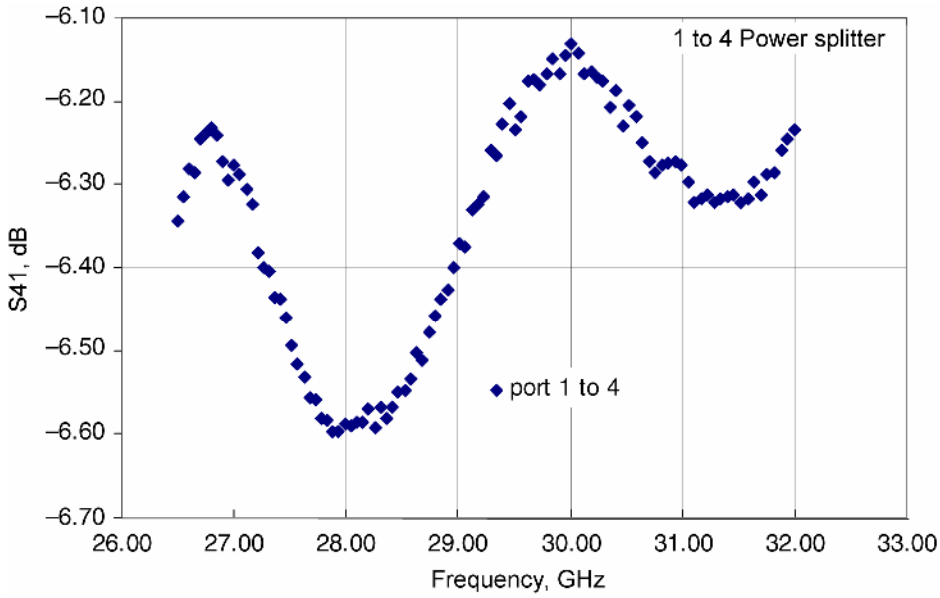

Figure 25.—The measured transmission to port #4. Narrow band sweep.

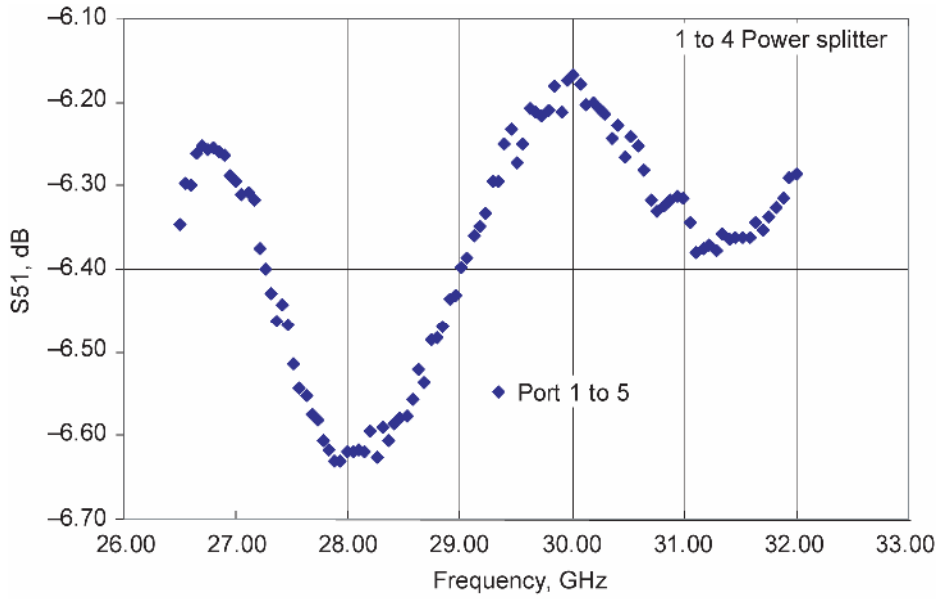

Figure 26.—Measured narrow band sweep of the transmission to port #5.

IX. Folded Magic-Tees With Improved Combining Efficiency

The above configurations can be designed for higher combining efficiency, improved power handling capability and compactness if the internal construction is modified and the ports are folded. Hence, a parallel investigation consisting of the computer modeling/simulation of novel magic-tee and alternative hybrid junction configurations were performed using CST Microwave Studio (ref. 21). The results showed that both the magic-tee and "folded E-plane" junctions could be designed for low loss (≈ 0.1 to 0.2 dB and >95 percent efficiency) and high power (kW) handling capability.

X. Comparison With Other Combiner Configurations

A power combining study was also performed under Project Prometheus by L-3 Communications (formerly Boeing) in which they investigated the use of magic-tee/hybrid couplers for the combination of 4, 5, 6, 7, and 8 high power amplifiers (TWTs) and also did a comparison between the magic-tee and the Jet Propulsion Laboratory (JPL) 5-way radial combiner design. Advantages of the magic-tee approach over the radial combiner include the following: extensive flight heritage vs. none; high power handling (2 kW at Ku-band-flying) versus uncertain; easy manufacturability vs. complex to design and manufacture and requirement for a mode converter; no overmoding; broader bandwidth; and lower insertion loss. The one advantage of the radial combiner is smaller volume. The recommendation of the study, based on consideration of cost, complexity and risk, was the use of either 4-way or 8-way magic-tee technology to generate several hundred watts of RF power. For 8 or fewer high power amplifiers (TWTs), the magic-T alone or magic-tee/hybrid combination was preferred to radial combining.

TABLE 3.— PORT CONFIGURATIONS AND ELECTRICAL SPECIFICATIONS OF THE MAGIC-TEE

Model Number		Millitech, Inc., CMT-28
Frequency Coverage (GHz)		26.5-38
Insertion Loss (dB) (max)		0.5
VSWR (max)	H-Arm Ports	1.5:1
	E-Arm Ports	1.6:1
Isolation (min) (dB)	E- to H-Arms	30
	Co-linear Arms	20
Balance ±dB (max)		0.5
Dimensions (in.)		1.5 by 1.5 by 1.5
Material		Aluminum

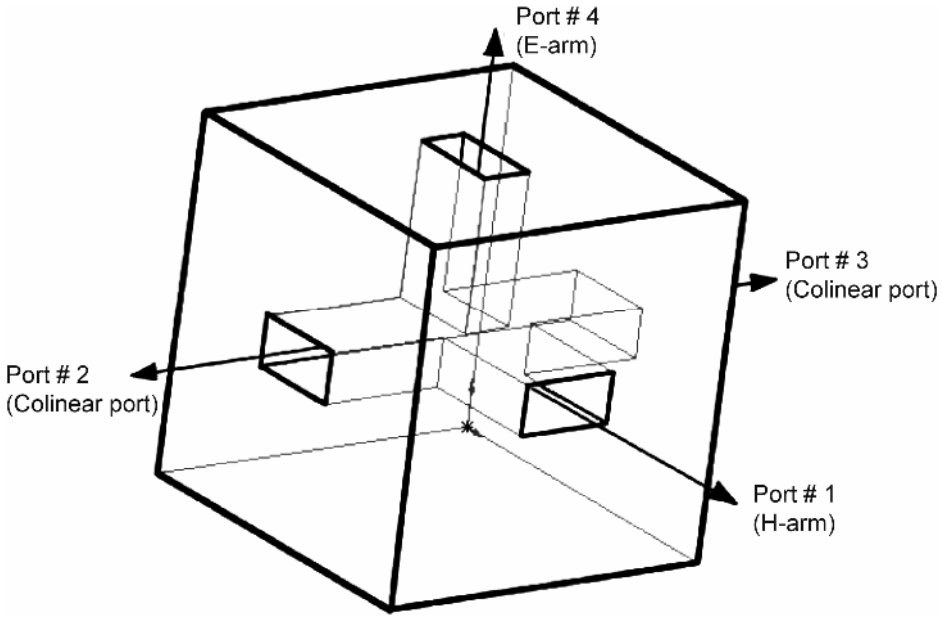

References

1. I.P. Smorchkova, et al. “AlGaN/GaN HEMT high-power and low-noise performance at f > 20 GHz,” IEEE Lester Eastman Conference, Proceedings on High Performance Devices, 2002, pp. 422–427.
2. I.P. Smorchkova, et al. “AlGaN/GaN HEMTs-Operation in the K-Band and Above,” IEEE Trans. Microwave Theory Tech., vol. 51, 2003, pp. 665–667.
3. J.S. Moon, et al. “GaN/AlGaN HEMTs operating at 20 GHz with continuous-wave power density > 6W/mm,” Electronics Letters, vol. 37, no.8, 2001, pp. 528–530.
4. R. Sandhu, et al. “3.2W/mm, 71% PAE AlGaN/GaN HEMT Operation at 20 GHz,” Device Research Conference Digest, 2002, June, pp. 27–28.
5. R. Sandhu, et al. “1.6 W/mm, 25% PAE AlGaN/GaN HEMT Operation at 29 GHz,” IEDM Technical Digest, 2001, pp. 17.5.1–17.5.3.
6. F. van Raay, et al. “Large Signal Modeling of AlGaN/GaN HEMTs with Psat> 4 W/mm at 30 GHz suitable for Broadband Power Applications,” 2003 IEEE MTT-S Digest, pp. 451–454.
7. R. Keifer, et al. “AlGaN/GaN-HEMTs for Power Applications up to 40 GHz,” IEEE Lester Eastman Conference, Proceedings on High Performance Devices, 2002, pp. 502–504.

8. C. Lee, et al. “AlGaN-GaN HEMTs on SiC with CW Power Performance of >4W/mm and 23% PAE at 35 GHz,” IEEE Electron Device Letters, vol. 24, October 2003, pp. 616–618.
9. J.S. Moon, et al. “Gate-Recessed AlGaN/GaN HEMTs for High-Performance Millimeter-Wave Applications,” IEEE Electron Device Letters, vol. 26, June 2005, pp. 348–350.
10. Y.F. Wu, et al. “3.5-Watt AlGaN/GaN HEMTs and Amplifiers at 35 GHz,” IEDM Technical Digest, 2003, pp. 23.5.1–23.5.3.
11. K. Kasahara, et al. “Ka-band 2.3W power AlGaN/GaN heterojunction FET,” IEDM Digest, 2002, pp. 677–680.
12. T. Palacios, et al. “High-Power AlGaN/GaN HEMTs For Ka-Band Applications,” IEEE Electron Device Letters, vol. 26, November 2005, pp. 781–783.
13. Special Issue on Wide Bandgap Semiconductor Devices and Circuits, IEEE Trans. Microwave Theory Tech., vol. 51, no. 2, part II, February 2003.
14. QuinStar Technology, Inc., Torrance, CA.
15. K. Chang and C. Sun, “Millimeter-Wave Power-Combining Techniques,” IEEE Trans. Microwave Theory Tech., vol. 31, no. 2, pp. 91–107, February 1983.
16. E.W. Bryerton, M.D. Weiss, and Z. Popovic, “Efficiency of Chip-Level Versus External Power Combining,” IEEE Trans. Microwave Theory Tech., vol. 47, no. 8, pp. 1482–1485, Aug. 1999.
17. P. Jia, L. Chen, A. Alexanian, and R. York, “Broad-Band High-Power Amplifier Using Spatial Power-Combining Technique,” IEEE Trans. Microwave Theory Tech., vol. 51, no. 12, pp. 2469–2475, December 2003.
18. L.W. Hendrick and R. Levy, “Design of Waveguide Narrow-Wall Short-Slot Couplers,” IEEE Trans. Microwave Theory Tech., vol. 48, no. 10, pp. 1771–1774, October 2000.
19. E.G. Wintucky, R.N. Simons, G.G. Lesny, J.L. Glass, “Waveguide Power Combiner Demonstration for Multiple High Power Millimeter Wave TWTAs,” Fifth IEEE Inter. Vacuum Electronics Conf. Dig. (IVEC 2004), pp. 98–99, Monterey, CA, April 27–29, 2004.
20. E.G. Wintucky, R.N. Simons, J.C. Freeman, A.J. Zaman, R.E. Jones, D.A. Carek, J.T. Bernhard, G.G. Lesny, and J.L. Glass, “Ka-Band Technology Developments for Space Communications at the NASA Glenn Research Center,” Proc. 10th Ka and Broadband Communications Conference, pp. 501–508, Vicenza, Italy, Sept. 30–Oct 2, 2004.
21. K.R. Vaden and R.N. Simons, “Computer Aided Design of Ka-Band Waveguide Power Combiner Architectures for Interplanetary Spacecraft,” 2005 IEEE Inter. Symp. on Antennas & Propagation & USNC/URSI National Radio Science Meet., pp. 635–638, vol. 1A, Washington, D.C., July 3–8, 2005. (Also NASA/TM—2006-214108.)

REPORT DOCUMENTATION PAGE

Form Approved
OMB No. 0704-0188

1. AGENCY USE ONLY (*Leave blank*)	2. REPORT DATE	3. REPORT TYPE AND DATES COVERED
	November 2006	Technical Memorandum

4. TITLE AND SUBTITLE

High Power High Efficiency Ka-Band Power Combiners for Solid-State Devices

5. FUNDING NUMBERS

WBS 122272.01.03.0473.01

6. AUTHOR(S)

Jon C. Freeman, Edwin G. Wintucky, and Christine T. Chevalier

7. PERFORMING ORGANIZATION NAME(S) AND ADDRESS(ES)

National Aeronautics and Space Administration
John H. Glenn Research Center at Lewis Field
Cleveland, Ohio 44135–3191

8. PERFORMING ORGANIZATION REPORT NUMBER

E–15710

9. SPONSORING/MONITORING AGENCY NAME(S) AND ADDRESS(ES)

National Aeronautics and Space Administration
Washington, DC 20546–0001

10. SPONSORING/MONITORING AGENCY REPORT NUMBER

NASA TM—2006-214447

11. SUPPLEMENTARY NOTES

Jon C. Freeman and Edwin G. Wintucky, NASA Glenn Research Center; and Christine Chevalier, Analex Corporation 1100 Apollo Drive, Brook Park, Ohio 44142. Responsible person, Jon C. Freeman, organization code RCE, 216–433–3380.

12a. DISTRIBUTION/AVAILABILITY STATEMENT

Unclassified - Unlimited
Subject Category: 33

Available electronically at http://gltrs.grc.nasa.gov

This publication is available from the NASA Center for AeroSpace Information, 301–621–0390.

12b. DISTRIBUTION CODE

13. ABSTRACT ***(Maximum 200 words)***

Wide-band power combining units for Ka-band are simulated for use as MMIC amplifier applications. Short-slot couplers as well as magic-tees are the basic elements for the combiners. Wide bandwidth (5 GHz) and low insertion (~0.2 dB) and high combining efficiencies (~90 percent) are obtained.

14. SUBJECT TERMS

Power combiners

15. NUMBER OF PAGES

28

16. PRICE CODE

17. SECURITY CLASSIFICATION OF REPORT	18. SECURITY CLASSIFICATION OF THIS PAGE	19. SECURITY CLASSIFICATION OF ABSTRACT	20. LIMITATION OF ABSTRACT
Unclassified	Unclassified	Unclassified	